Overview of Techniques for the Detection and Characterization of Exoplanets

Dmitry Savransky

Cornell University

Carl Sagan Institute

SIOS Laboratory

Solar system barycenter at O, exosystem barycenter at G. S is star position at time t and point c is the (time-varying) position of the centroid of a group of reference stars.

$$\hat{\mathbf{r}}_{S/O}(t_0) \equiv \mathbf{b}_3 = \begin{bmatrix} \cos\lambda\cos\beta \\ \sin\lambda\cos\beta \\ \sin\beta \end{bmatrix}_{\mathcal{I}}$$

$$\mathbf{b}_1 = \begin{bmatrix} -\sin\lambda \\ \cos\lambda \\ 0 \end{bmatrix}_{\mathcal{I}}$$

$$\mathbf{b}_2 = \begin{bmatrix} -\cos\lambda\sin\beta \\ -\sin\lambda\sin\beta \\ \cos\beta \end{bmatrix}_{\mathcal{I}}$$

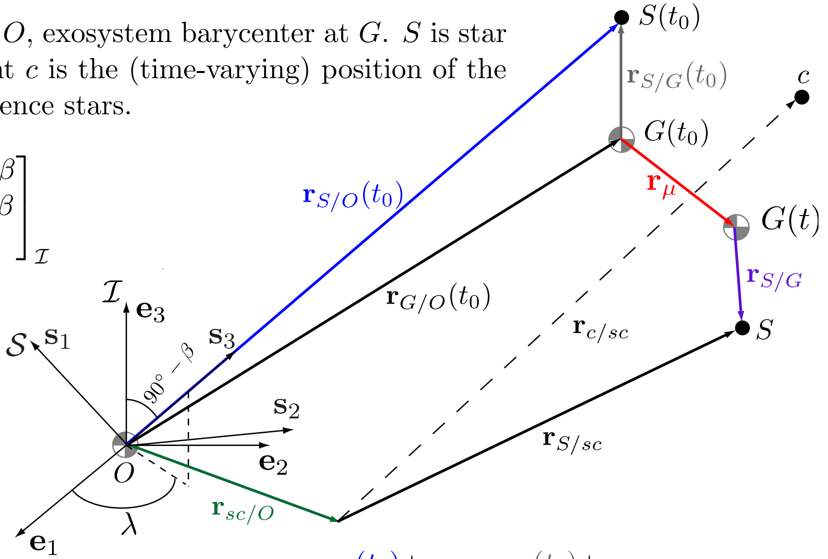

$$\mathbf{r}_{S/sc} = \mathbf{r}_{S/O}(t_0) + \mathbf{r}_\mu - \mathbf{r}_{S/G}(t_0) + \mathbf{r}_{S/G} - \mathbf{r}_{sc/O}$$

Astrometry

- $\mathbf{r}_\mu$ is the motion of the exosystem barycenter, with components approximated as constants: $\mathbf{r}_\mu(t) = \sigma_x \mathbf{b}_1 + \sigma_y \mathbf{b}_2 + \sigma_z \hat{\mathbf{r}}_s(t_0)$
- Split barycenter velocity into transverse and radial velocities:

$$\frac{{}^{\mathcal{I}}\mathrm{d}}{\mathrm{d}t}\mathbf{r}_{G/O}(t) \equiv \frac{{}^{\mathcal{I}}\mathrm{d}}{\mathrm{d}t}\left(\mathbf{r}_{G/O}(t_0) + \mathbf{r}_\mu(t)\right) = \frac{{}^{\mathcal{I}}\mathrm{d}}{\mathrm{d}t}\mathbf{r}_\mu(t)$$

$$= V_R \hat{\mathbf{r}}_{S/O}(t_0) + \mathbf{V}_T \quad \text{where}$$

$$\mathbf{V}_T = \hat{\mathbf{r}}_{S/O}(t_0) \times \left(\frac{{}^{\mathcal{I}}\mathrm{d}}{\mathrm{d}t}\mathbf{r}_{G/O}(t) \times \hat{\mathbf{r}}_{S/O}(t_0)\right)$$

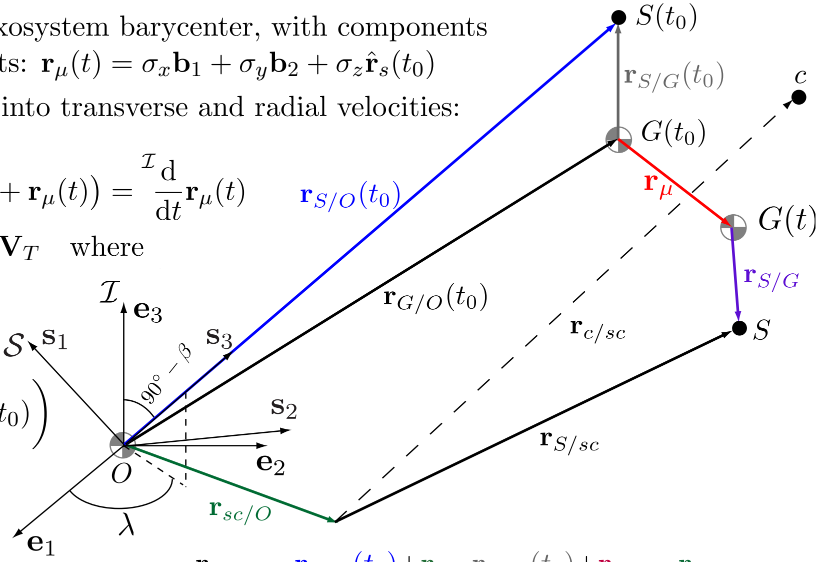

$$\mathbf{r}_{S/sc} = \mathbf{r}_{S/O}(t_0) + \mathbf{r}_\mu - \mathbf{r}_{S/G}(t_0) + \mathbf{r}_{S/G} - \mathbf{r}_{sc/O}$$

Interferometric Astrometry

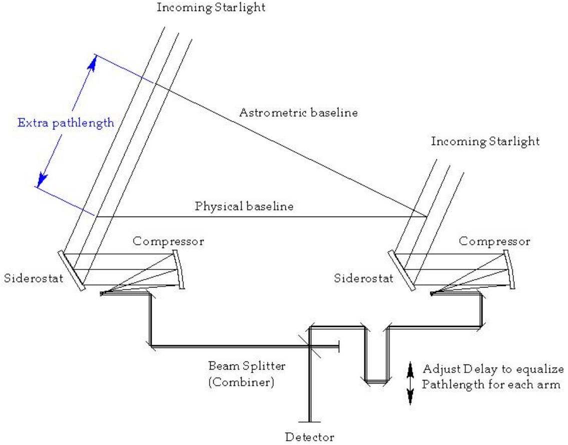

Image Credit: NASA

$$\text{OPD} = \mathbf{B} \cdot \hat{\mathbf{r}}_{S/sc} + k + \text{noise}$$

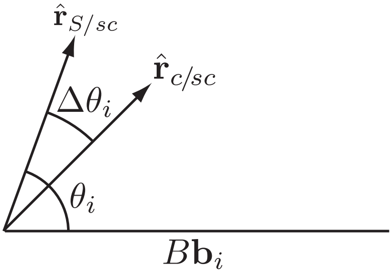

$$d_i = B\left(\cos\theta_i - \cos(\theta_i - \Delta\theta_i)\right)$$
$$\approx -B\sin\theta_i \Delta\theta_i$$

Doppler Spectroscopy

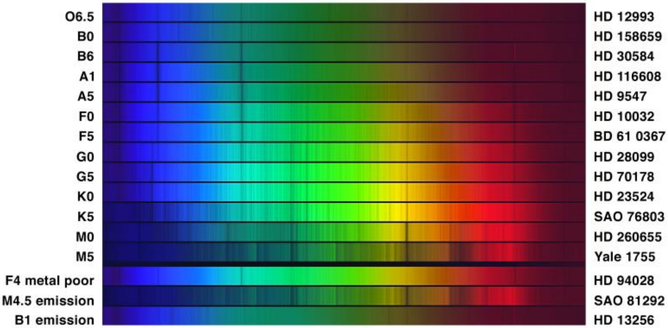

Image Credit: NOAO

$$I_{obs}(\lambda) = \kappa\left[I_S(\lambda + \Delta\lambda_S)T_C(\lambda + \Delta\lambda_C)\right] \otimes \mathrm{PSF}$$

$$\Delta\lambda = \Delta\lambda_S - \Delta\lambda_C$$

$$\frac{\Delta\lambda}{\lambda} = \frac{(1+\rho_g)}{n}\sqrt{\frac{\left(1+\frac{v}{c}\right)}{1-\frac{v}{c}}} - 1$$

ρ_g: Gravitational redshift of starlight

n: Index of refraction of air column

$$v \ll c \quad \Rightarrow \quad \frac{\Delta\lambda}{\lambda} \approx \frac{v}{c}$$

$$v = \|{}^{\mathcal{I}}\mathbf{v}_{S/sc}\|$$

Sometimes You Have to Be Lucky

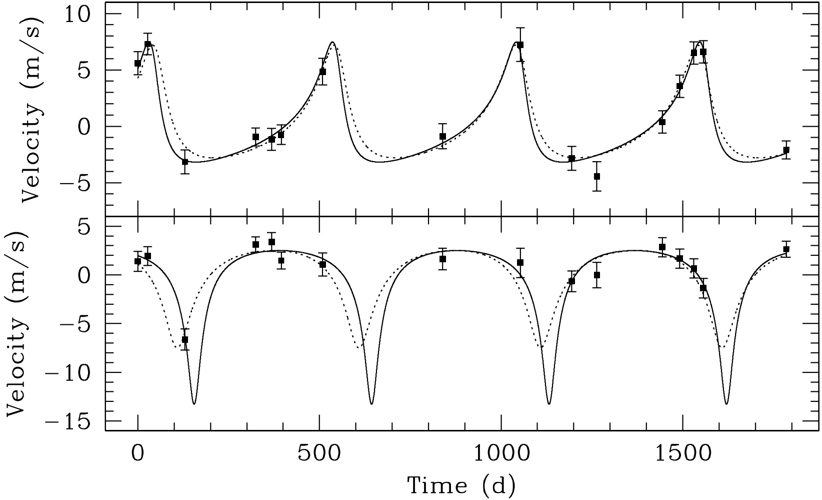

From: Cumming et al. (2004). True orbit (dashed), Best fit (solid). Top panel detected, bottom not.

RV is Only Sensitive to a Subset of Keplerian Elements

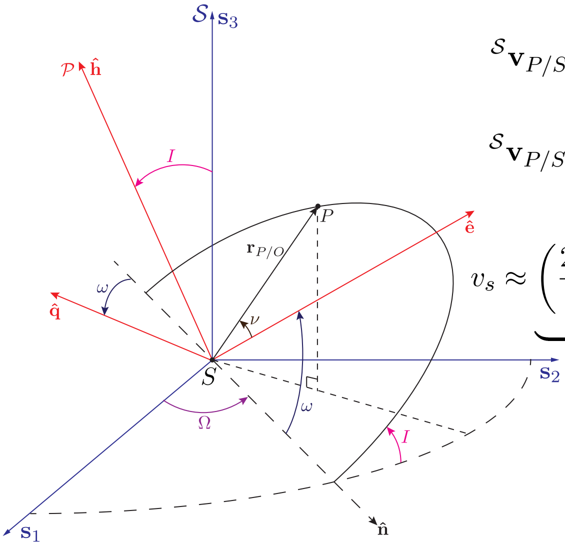

$$^{\mathcal{S}}\mathbf{v}_{P/S} = \sqrt{\frac{\mu}{\ell}}\left(-\sin\nu\hat{\mathbf{e}} + (e+\cos\nu)\hat{\mathbf{q}}\right)$$

$$^{\mathcal{S}}\mathbf{v}_{P/S}\cdot\mathbf{s}_3 = \sqrt{\frac{\mu}{a}}\sqrt{\frac{1}{1-e^2}}\sin(I)\left(e\cos(\omega)+\cos(\nu+\omega)\right)$$

$$v_s \approx \underbrace{\left(\frac{2\pi G}{T_P}\right)^{\frac{1}{3}}\frac{m_P\sin(I)}{m_S^{\frac{2}{3}}}\frac{1}{\sqrt{1-e^2}}}_{\triangleq K}\left(e\cos(\omega)+\cos(\nu+\omega)\right)$$

Can independently fit

$\omega, \nu, e, T_P, m_P\sin(I)$

$\Omega, \omega \sim U([0, 2\pi])$ $\quad I \sim \cos^{-1}\left(U([-1,1])\right)$

Transit Photometry

$$\frac{F_S^{(e)}}{F_S} = \begin{cases} 1 & R_S + R < s \\ 1 - \frac{1}{\pi}\left[\frac{R^2}{R_S^2}\kappa_0 + \kappa_1 - \sqrt{\frac{s^2}{R_S^2} - \frac{\left(R_S^2+s^2-R^2\right)^2}{4R_S^4}}\right] & \lvert R_S - R\rvert < s \leq R_S + R \\ 1 - \left(\frac{R}{R_S}\right)^2 & s \leq R_S - R \\ 0 & s \leq R - R_S \end{cases}$$

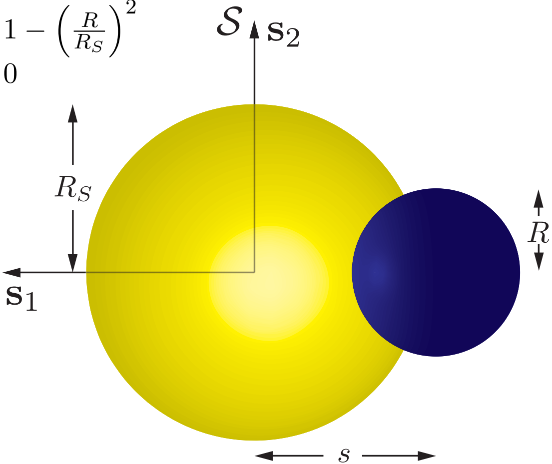

$$\kappa_0 = \cos^{-1}\left(\frac{R^2 + s^2 - R_S^2}{2Rs}\right)$$

$$\kappa_1 = \cos^{-1}\left(\frac{R_S^2 - R^2 + s^2}{2R_S s}\right)$$

Lots of Other Effects to Model

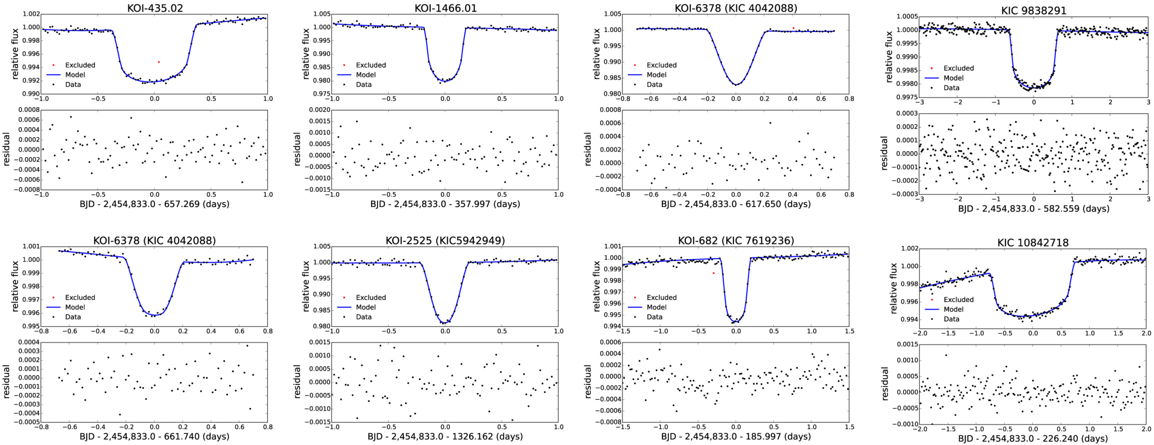

From: Aizawa et al. (2017)

Gravitational Microlensing

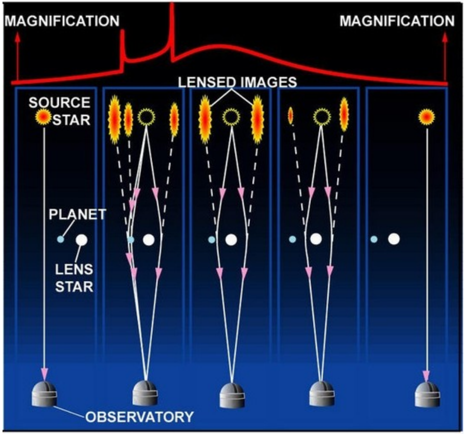

Image Credit: OGLE

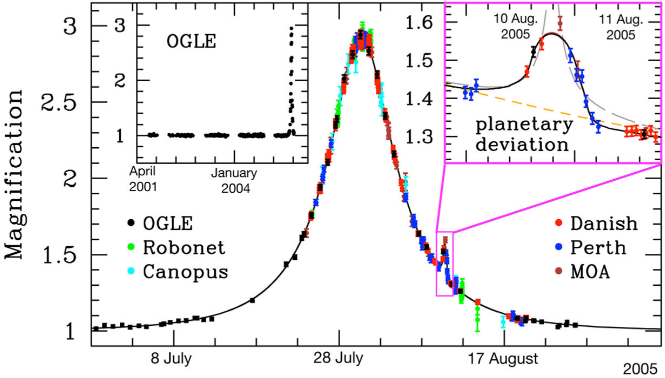

Light curve of OGLE-2005-BLG-390.
Image Credit: ESO

Exosystem Geometry

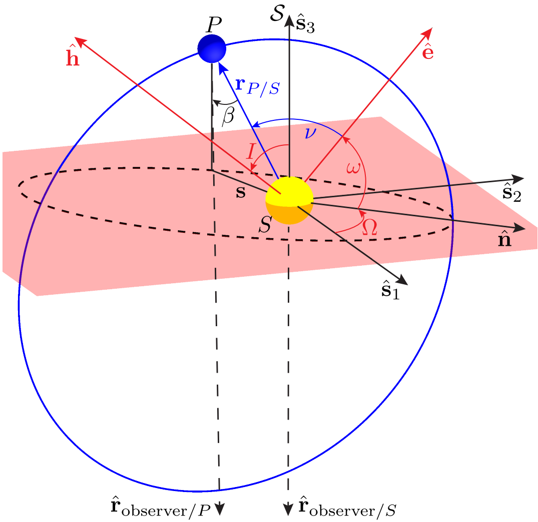

a	Semi-major axis
ν	True anomaly
e	Eccentricity
$\mathbf{s}$	Projected separation
$\mathbf{r}_{P/S}$	Orbital radius vector
	$= r\left(\cos\nu\hat{\mathbf{e}} + \sin\nu\hat{\mathbf{q}}\right)$
r	Orbital radius
	$= \lVert\mathbf{r}_{P/S}\rVert = \dfrac{a(1-e^2)}{e\cos(\nu)+1}$
β	Phase (star-planet-observer) angle
	$\approx \cos^{-1}\left(\dfrac{\mathbf{r}_{P/S}\cdot\hat{\mathbf{s}}_3}{r}\right)$
	$= \cos^{-1}\left(\sin(I)\sin(\omega+\nu)\right)$

Exosystem Geometry

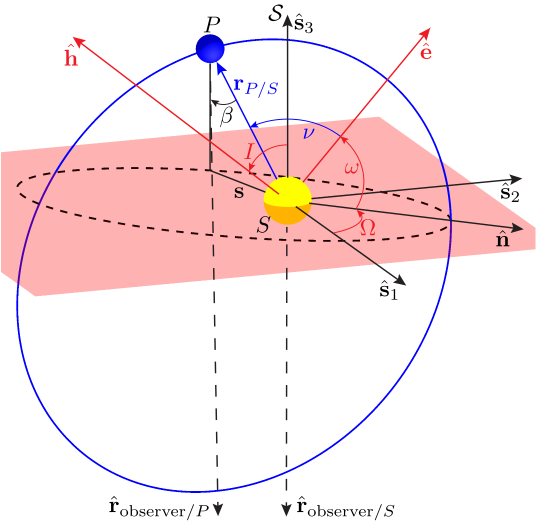

a	Semi-major axis
ν	True anomaly
e	Eccentricity
$\mathbf{s}$	Projected separation
$\mathbf{r}_{P/S}$	Orbital radius vector
	$= r\left(\cos\nu\hat{\mathbf{e}} + \sin\nu\hat{\mathbf{q}}\right)$
r	Orbital radius
	$= \Vert\mathbf{r}_{P/S}\Vert = \dfrac{a(1-e^2)}{e\cos(\nu)+1}$
β	Phase (star-planet-observer) angle
	$\approx \cos^{-1}\left(\dfrac{\mathbf{r}_{P/S}\cdot\hat{\mathbf{s}}_3}{r}\right)$
	$= \cos^{-1}\left(\sin(I)\sin(\omega+\nu)\right)$
	$\Rightarrow \hat{\mathbf{r}}_{sc/P} \parallel \hat{\mathbf{r}}_{sc/S}$

Imaging Constraints

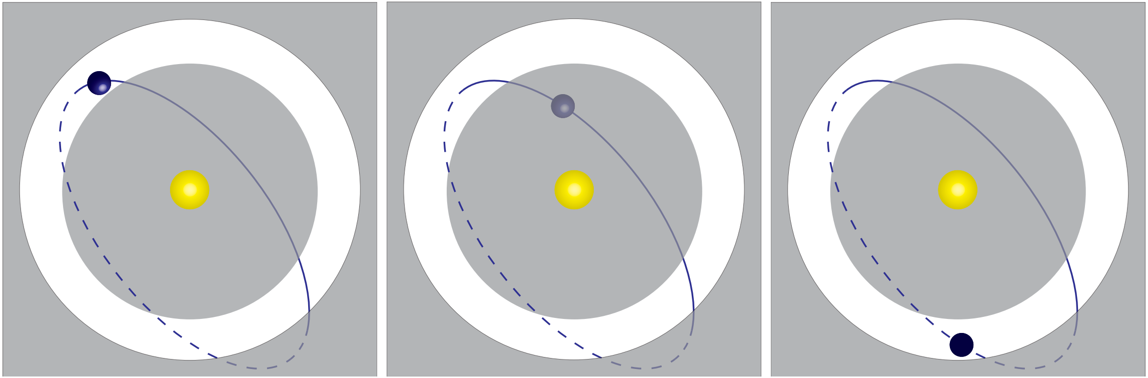

Schematic of projected exosystem. Planet is sufficiently illuminated for detection in reflected light on solid part of orbit, and observable outside the gray region.

All imaging systems have an inner/outer working angle (IWA/OWA) and a limiting planet/star flux ratio (function of angular separation).

Reflected Light

Energy per second per unit area per unit solid angle received by an observer =

$$\frac{FR^2}{r^2}\int_{\beta-\pi/2}^{\pi/2}\cos(\beta-\delta)\cos\delta\,\mathrm{d}\delta\int_{-\pi/2}^{\pi/2}\rho(C_\mu,C_\gamma,\xi)\cos^3\alpha\,\mathrm{d}\alpha$$

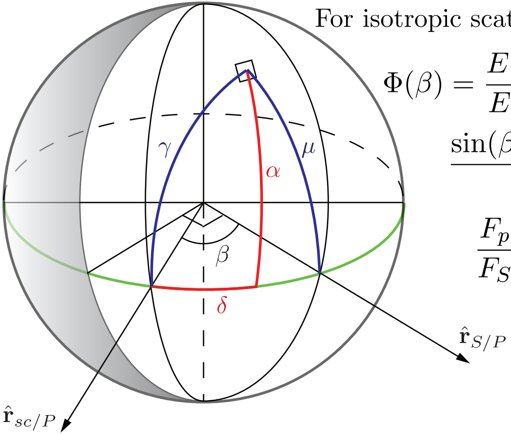

For isotropic scattering, ρ = constant

$$\Phi(\beta) = \frac{E(\beta)}{E(0)} = \frac{\sin(\beta) + (\pi-\beta)\cos(\beta)}{\pi}$$

$$\frac{F_p}{F_S} = p\Phi(\beta)\left(\frac{R}{r}\right)^2$$

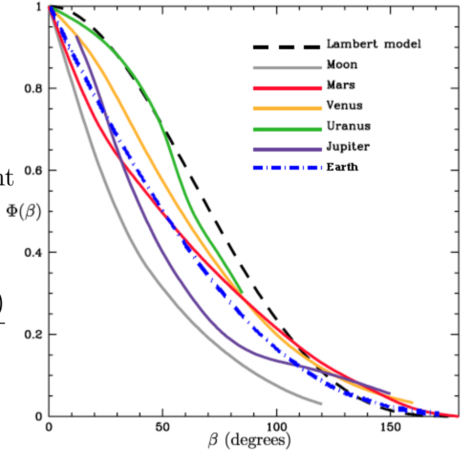

Solar system body and isotropic-scatterer (Lambert) phase functions. Data from Sudarsky et al. (2005) and De Vaucouleurs (1964)

Thermal Emission

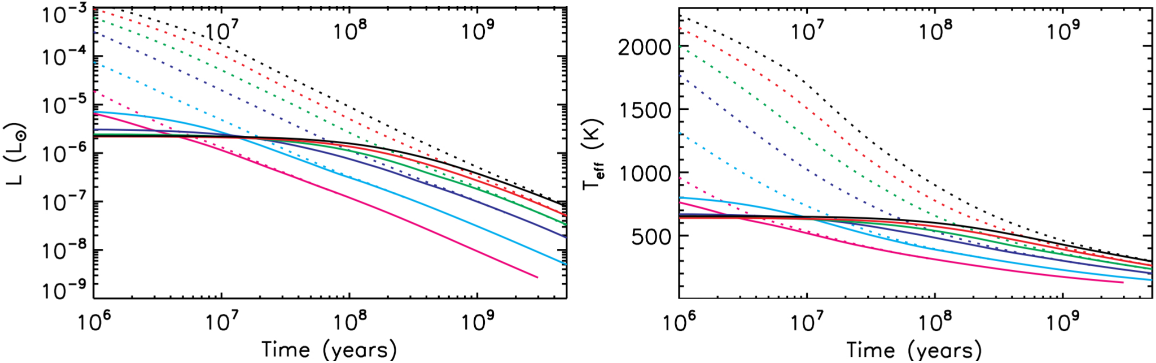

From: Marley et al. (2007). Dotted lines represent hot-start evolution and solid lines represent core-accretion evolution.

Clouds Complicate Things

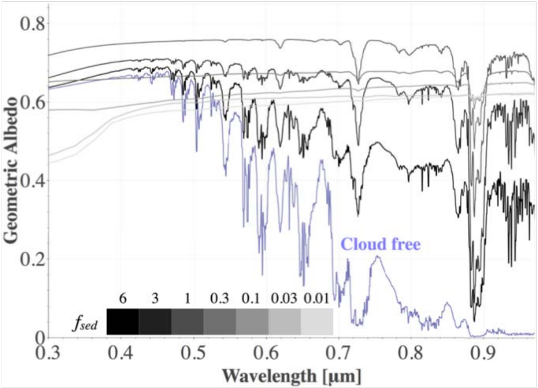

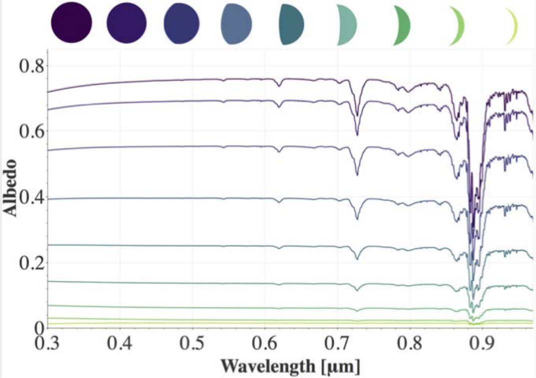

From: Batalha et al., "Color Classification of Extrasolar Giant Planets: Prospects and Cautions", 2018

Spectroscopy

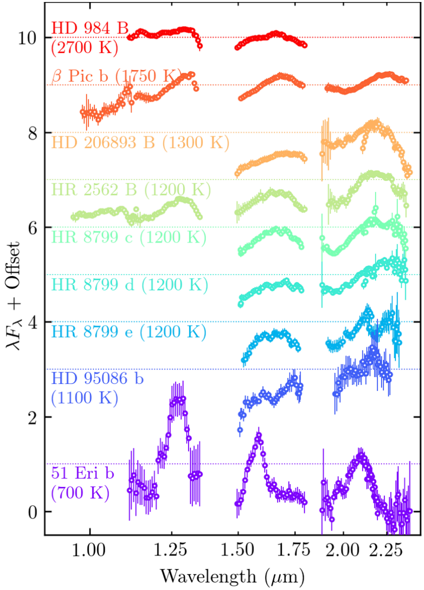

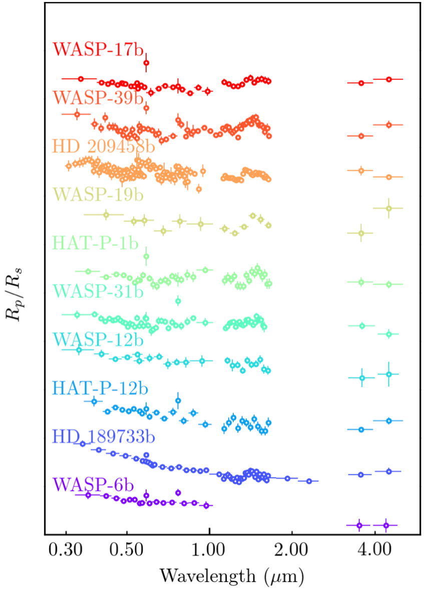

Left: Ground-based imaging spectral library from GPIES.
Right: Transit spectroscopy spectra from HST and Sptizer (Sing et al. 2016).

Conventional Telescopes Are Not Conducive to Imaging Planets

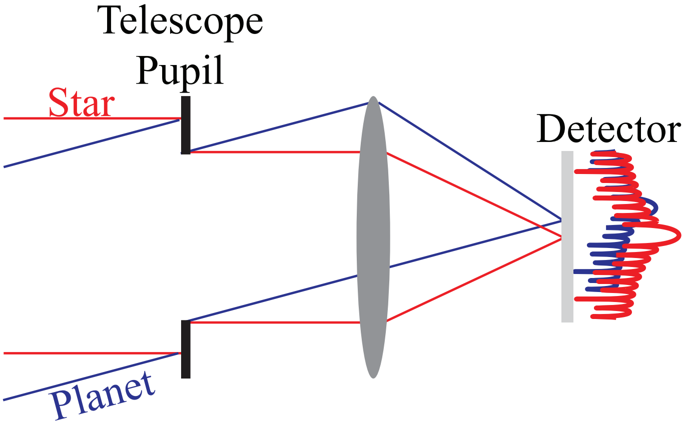

Telescope schematic: a finite-sized aperture captures light that is focused onto a detector.

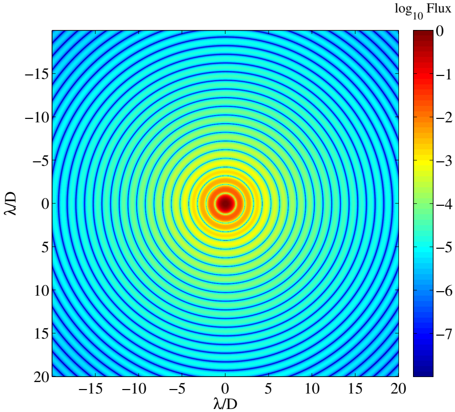

The system impulse response (Point Spread Function) in log scale

In 1931 Astronomers Got Tired of Chasing Eclipses

Photo by Miloslav Druckmüller

In 1931 Astronomers Got Tired of Chasing Eclipses

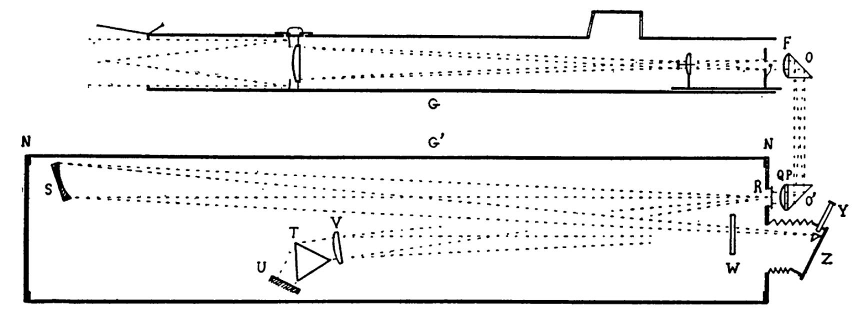

The first Lyot Coronagraph.
Lyot (1939)

Photo by Miloslav Druckmüller

Coronagraphy 101

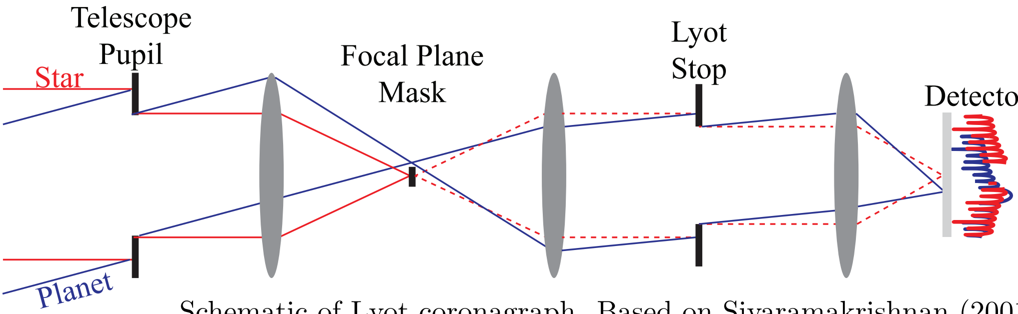

Schematic of Lyot coronagraph. Based on Sivaramakrishnan (2001).

Coronagraphy 101

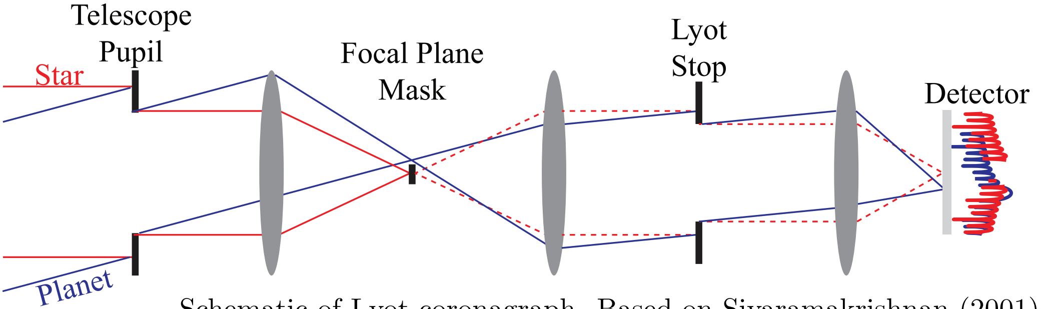

Schematic of Lyot coronagraph. Based on Sivaramakrishnan (2001).

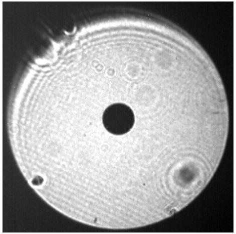

Pupil

Coronagraphy 101

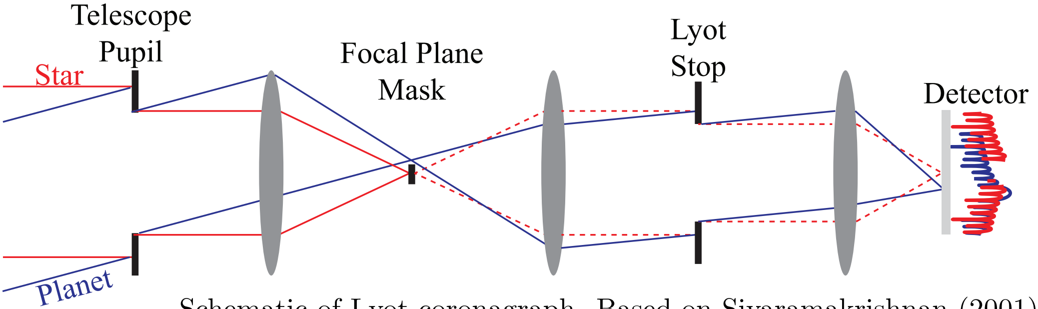

Schematic of Lyot coronagraph. Based on Sivaramakrishnan (2001).

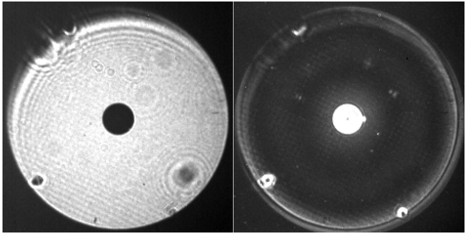

Pupil FPM

Coronagraphy 101

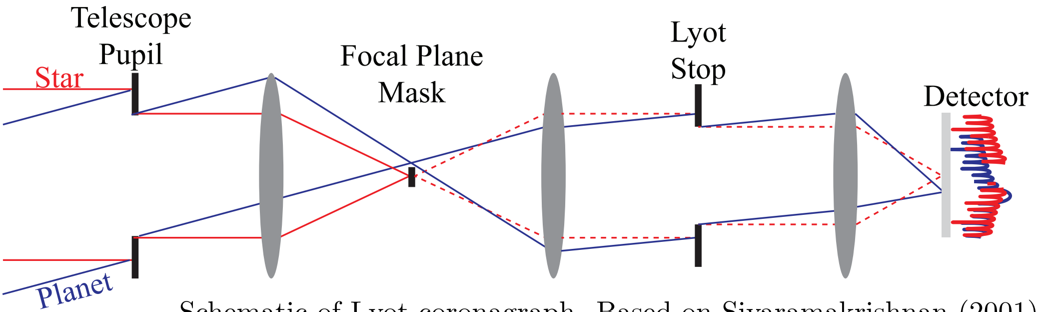

Schematic of Lyot coronagraph. Based on Sivaramakrishnan (2001).

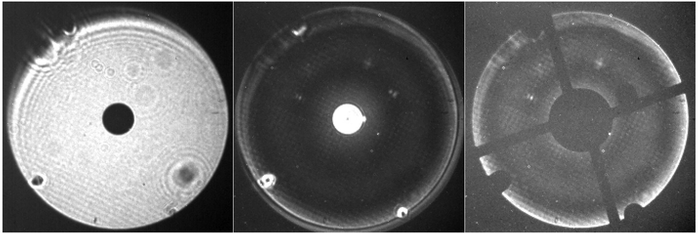

Pupil FPM FPM+Lyot

Apodized Pupil Lyot Coronagraphy

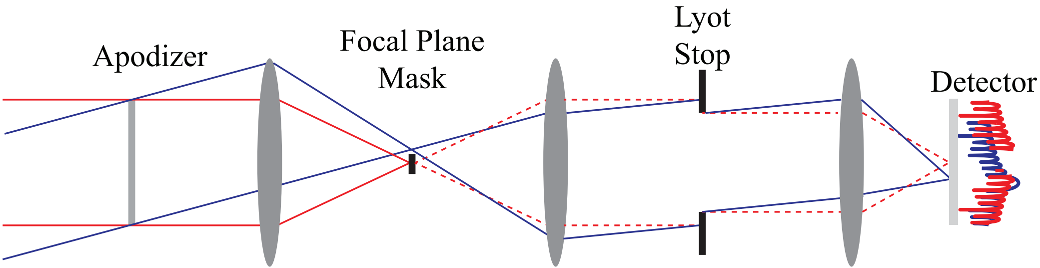

Schematic of Lyot coronagraph. Based on Sivaramakrishnan (2001).

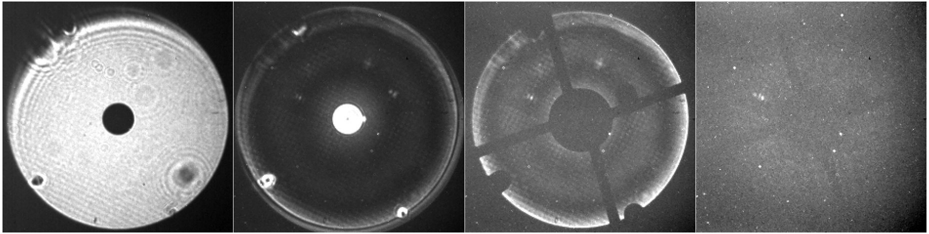

Pupil FPM FPM+Lyot +Apodizer

Pre-apodize to remove residual diffraction

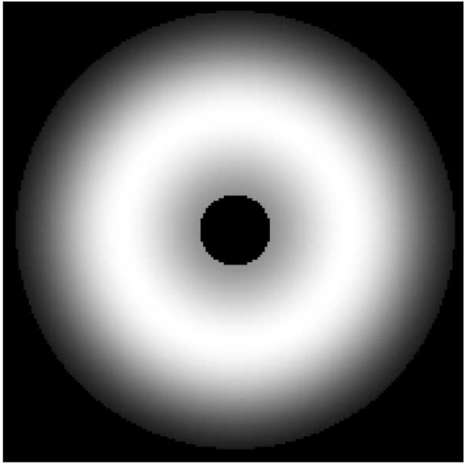

(a) Apodizer function

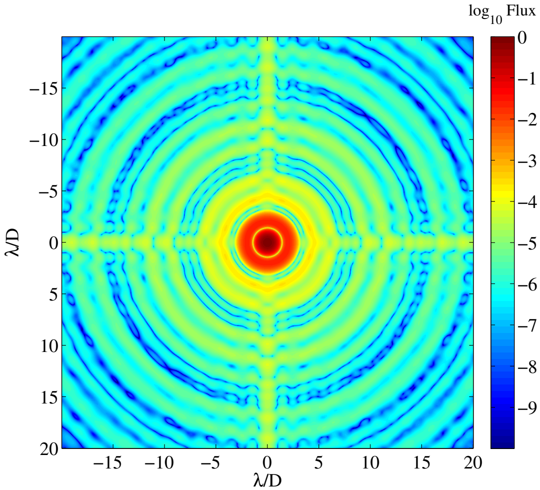

(b) Point Spread Function

“Apodized Pupil Lyot Coronagraphs for Arbitrary Telescope Apertures”, Soummer et al. (2004)

Shaped Pupil Coronagraphy

Alternatively, you can reshape the Point Spread Function completely:

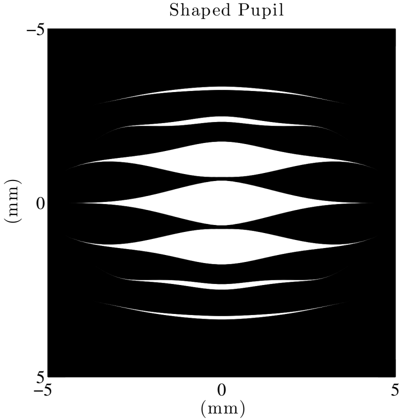

(a) Pupil Mask

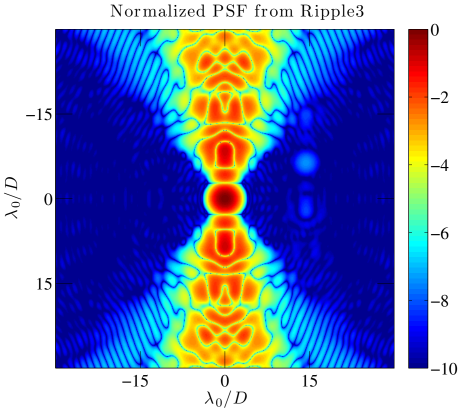

(b) Point Spread Function

Images courtesy of T. Groff. See: "Optimal one-dimensional apodizations and shaped pupils for planet finding coronagraphy", Kasdin et al. (2005)

Phase Mask Coronagraphy

Or use a phase-shift mask to produce destructive interference of the on-axis light:

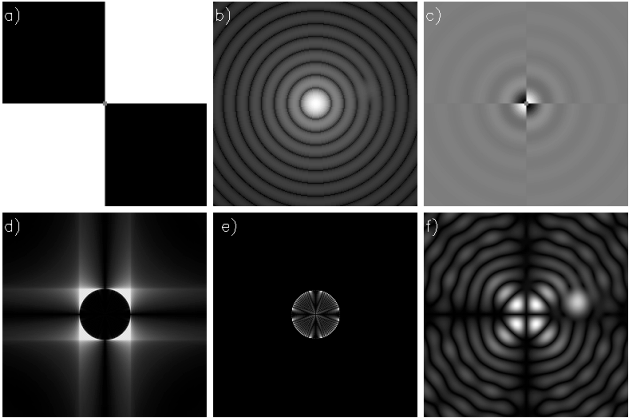

Figure: Four-quadrant phase mask and resulting PSFs. From Rouan et al. (2000)

See: "Stellar Coronagraph with Phase Mask", Roddier and Roddier (1997)

Phase-Induced Amplitude Apodization Coronagraphy

Or, instead of an apodizer mask, achieve your apodization via geometrical redistribution of the light (pupil-mapping). "Exoplanet Imaging with a Phase-Induced Amplitude Apodization Coronagraph", Guyon (2005)

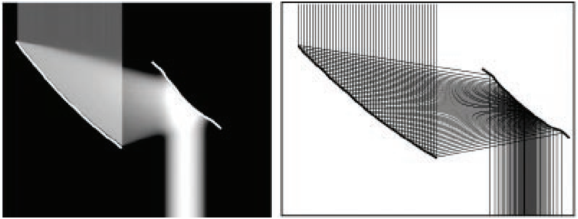

Figure: Intensity and ray trace of remapping mirrors.

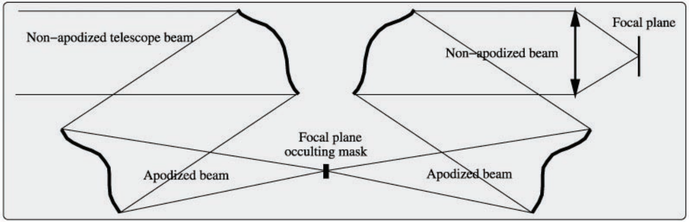

Figure: PIAAC schematic.

What If You Block the Light Outside the Telescope?

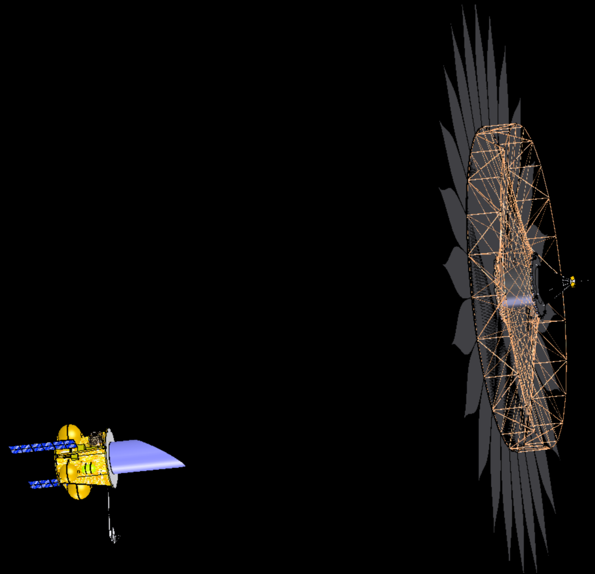

With the Right Shape, You Get a Deep Shadow

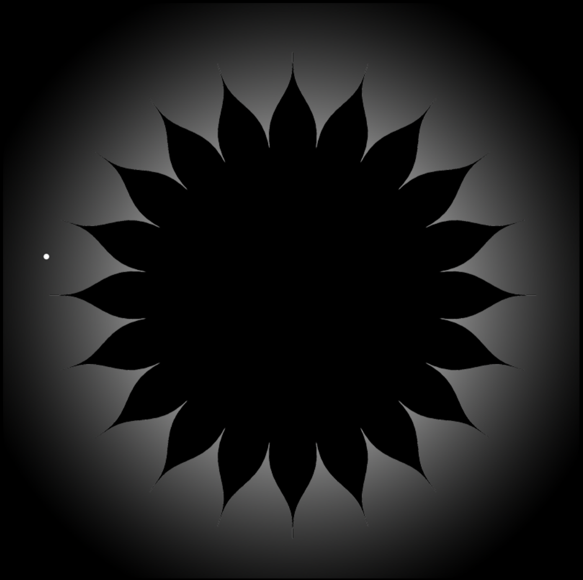

Why Would This Work?

Babinet's Principle

The light passing around the occulter plus the light passing through an occulter-shaped hole is a free-space plane wave.

You can design your occulter to produce the shadow you want at the telescope aperture (with no Poisson spot). See Vanderbei et al. (2007).

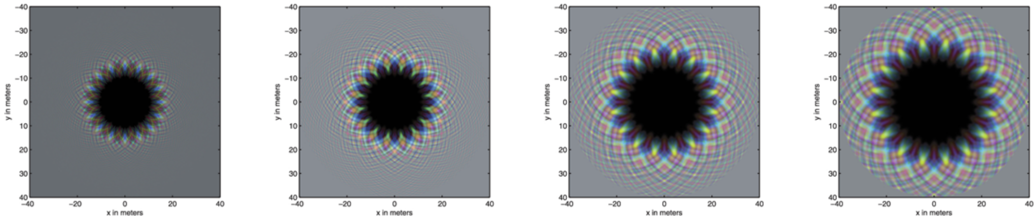

Figure: Simulated shadow cast at the telescope pupil for separations of 18 to 100 thousand km.

Minimum angular separation is now a function only of geometry, not wavelength!

Starshade Concepts

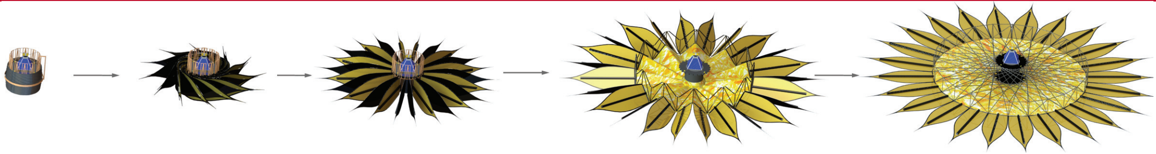

Figure: Starshade deployment concept. Thomson et al. (2011)

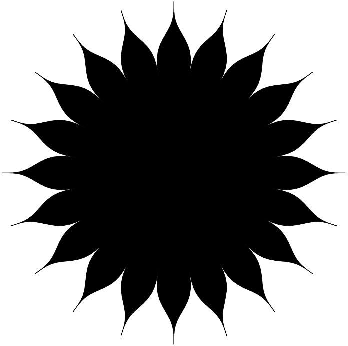

(a) THEIA starshade

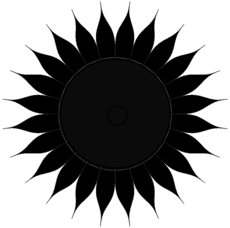

(b) O_3 starshade

What We Know Today